

Structure and pinning centres in MgB₂ bulk, wires and thin films and in MT-YBCO**

**T. Prikhna,^{1,*} A. Mamalis,² V. Romaka,³ M. Eisterer,⁴ J. Rabier,⁵
A. Jouline,⁵ V. Moshchil,¹ S. Ponomaryov,⁶ M. Rindfleisch,⁷
M. Tomsic,⁷ X. Chaud,⁸ A. Shapovalov,¹ A. Kozyrev,¹ A. Shaternik,¹
E. Prisyazhnaya¹ and Ch. Yang⁹**

¹ *V. Bakul Institute for Superhard Materials of the National Academy of Sciences of Ukraine (NASU), 2 Avtozavodskaya St, Kiev 07074, Ukraine*

² *Project Centre for Nanotechnology and Advanced Engineering, NCSR “Demokritos”, Athens, Greece*

³ *Atominstitut, TU Wien, Stadionallee 2, 1020 Vienna, Austria*

⁴ *Leibniz Institute for Solid State and Materials Research (IFW Dresden), Helmholtz St 20, 01069 Dresden, Germany*

⁵ *PHYMAT, UMR 6630, CNRS Université de Poitiers, SP2MI, BP 30179, 86962 Futuroscope, France*

⁶ *Institute of Semiconductor Physics of the National Academy of Sciences of Ukraine (NASU), 41, Nauky Ave, Kiev 03028, Ukraine*

⁷ *Hyper Tech Research, Inc., 539 Industrial Mile Road, Columbus, Ohio, USA*

⁸ *Laboratoire National des Champs Magnétiques Intenses (LNCMI/CNRS), 25 Avenue des Martyrs, BP 166, 38042 Grenoble Cedex 9, France*

⁹ *Harbin Institute of Technology, 92 West Dashi St, Harbin 1500001, China*

The structure and composition of MgB₂-based materials (bulk, wires and thin films) prepared at different pressures (0.1 MPa–2 GPa) and temperatures (600–1050 °C), and melt-textured YBa₂Cu₃O_{7-δ} (MT-YBCO) oxidized in oxygen flow at 440 °C and under hydrostatic pressure of 16 MPa at 800 °C, which demonstrated high critical current densities j_c , were analysed by X-rays, SEM–EDX and TEM. Correlations between the character of material inhomogeneities, which can be pinning centres and influence superconducting characteristics, are discussed. The effect of defects such as twins, dislocations, macrocracks and microcracks on critical current density and mechanical

* Corresponding author. E-mail address: prikhn@ukr.net

** This paper was first presented at the eleventh Japanese–Mediterranean workshop (JAPMED’11), 15–19 July 2019 in Batumi, Georgia.

characteristics of MT-YBCO is considered. Regularly distributed nanostructural inhomogeneities responsible for pinning and connected with Mg, B and O content variation in the nanoscale were observed in all types of the MgB₂-based materials. The effect of homogeneity of the matrix phase of MgB₂ wires, with and without additions of carbon and dysprosium oxide, as well as the ratio of Mg to B on the critical current densities in the wires, were established.

Keywords: electron microscopy, mechanical characteristics, MgB₂, superconducting materials, YBa₂Cu₃O_{7-δ}

1. Introduction

Superconducting (SC) materials based on MgB₂ and YBa₂Cu₃O_{7-δ} (YBCO) are promising for many different applications, such as fault current limiters, magnetic resonance imaging, SC magnetic energy storage devices, transformers, electrical motors and generators, cryogenic pumps, adiabatic demagnetization refrigerators, magnetic separators, magnetic levitation transport and bearings, and magnets for high-energy physics.¹⁻⁹ SC MgB₂ wires are used for aviation and space applications and for powerful offshore wind generators, etc.

The SC characteristics of MgB₂- and YBa₂Cu₃O_{7-δ}-based materials, such as critical current density, irreversibility field and trapped magnetic field, depend on the pinning of vortices by nanostructural defects commensurable with the coherence length (0.6–3.1 nm for Y123¹⁰ and 1.6–12 nm for MgB₂¹¹). Because of its comparatively high coherence length, high critical

- ¹ M. Tomsic, M. Rindfleisch, J. Yue, K. McFadden, J. Phillips, M.D. Sumption, M. Bhatia, S. Bohnenstiehl, E.W. Collings, Overview of MgB₂ superconductor applications. *Intl J. Appl. Ceram. Technol.* **4** (2007) 250–259.
- ² A. Ballarino, R. Flükiger, Status of MgB₂ wire and cable applications in Europe. *J. Phys.: Conf. Ser.* **871** (2017) 012098.
- ³ X. Obradors, T. Puig, Coated conductors for power applications: materials challenges. *Superconductor Sci. Technol.* **27** (2014) 044003.
- ⁴ V. Meerovich, V. Sokolovsky, T. Prikhna, W. Gawalek, T. Habisreuther, AC losses in high pressure synthesized MgB₂ bulk rings measured by a transformer method. *Superconductor Sci. Technol.* **26** (2011) 035015.
- ⁵ T. Prikhna, W. Gawalek, Ya. Savchuk, N. Sergienko, V. Moshchil, S. Dub, V. Sverdun, L. Kovalev, V. Penkin, O. Rozenberg, M. Zeisberger, M. Wendt, G. Fuchs, Ch. Grovenor, S. Haigh, V. Melnikov, P. Nagorny, High-pressure high-temperature synthesis of nanostructural magnesium diboride for electromotors and devices working at liquid hydrogen temperatures. *Adv. Sci. Technol.* **47** (2006) 25–30.
- ⁶ U. Floegel-Delor, P. Schirrmeister, T. Riedel, R. Koenig, V. Kantarbar, F.N. Werfel, Bulk superconductor levitation devices: advances in and prospects for development. *IEEE Trans. Appl. Superconductivity* **28** (2018) 2809467.
- ⁷ F.N. Werfel, U. Floegel-Delor, R. Rothfeld, T. Riedel, P. Schirrmeister, R. Koenig, Experiments of superconducting maglev ground transportation. *IEEE Trans. Appl. Superconductivity* **26** (2016) 3602105.
- ⁸ R.M. Scanlan, A.P. Malozemoff, D.C. Larbalestier, Superconducting materials for large-scale applications. *Proc. IEEE* **92** (2004) 1639–1654.
- ⁹ P.T. Putman, Y.X. Zhou, H. Fang, A. Klawitter, K. Salama, Application of melt-textured YBCO to electromagnetic launchers. *Superconductor Sci. Technol.* **18** (2005) S6–S9.
- ¹⁰ D.A. Cardwell, D.S. Ginley, *Handbook of Superconducting Materials*. Bristol: Institute of Physics Publishing (2003).
- ¹¹ C. Buzea, T. Yamashita, Review of the superconducting properties of MgB₂. *Superconductor Sci. Technol.* **14** (2001) R115–R146.

currents can be realized in nanostructured MgB_2 ; grain boundaries and nanosized inclusions of secondary phases are considered as pinning centres.^{12,13} The boundaries between $YBa_2Cu_3O_{7-\delta}$ (or Y123) grains that are misoriented by more than $4\text{--}5^\circ$ are essential obstacles for SC current flow. Thus, for attaining high current densities and trapped magnetic fields, single-domain textured blocks or epitaxial films with no lattice mismatches have to be prepared. In melt-textured materials based on $YBa_2Cu_3O_{7-\delta}$ (MT-YBCO), pinning centres can be dislocations, stacking faults and twins, which are considered to play an important role on attaining high critical superconducting currents.^{14–21} Regularly distributed nanostructural inhomogeneities connected with Mg, B and O content variation on the nanolevel were observed in all types of the MgB_2 -based materials and are considered to be responsible for pinning in these materials. Application of pressure during the manufacturing process (gaseous oxygen pressure in the case of $YBa_2Cu_3O_{7-\delta}$ -based materials or mechanically created pressure in the case of MgB_2 -based) is of great help in attaining high functional SC characteristics of the materials. High pressure (2 GPa) processing, hot pressing (30 MPa), spark plasma (50 MPa) sintering or synthesis, explosive compaction and extrusion using the powder-in-tube method of MgB_2 as well as high pressure (10–16 MPa) and high temperature (700–800 °C) oxygenation of MT-YBCO can be successfully used for manufacturing stable materials with record superconductive and mechanical characteristics.^{22–27}

¹² M. Eisterer, Magnetic properties and critical currents of MgB_2 . *Superconductor Sci. Technol.* **20** (2007) R47–R73.

¹³ E.W. Collings, M.D. Sumption, M. Bhatia, M.A. Susner, S.D. Bohnenstiehl, Topical review: Prospects for improving the intrinsic and extrinsic properties of magnesium diboride superconducting strands. *Superconductor Sci. Technol.* **21** (2008) 103001.

¹⁴ K. Salama, O.F. Lee, Progress in melt texturing of $YBa_2Cu_3O_x$ superconductor. *Superconductor Sci. Technol.* **7** (1994) 177–193.

¹⁵ J. Plain, T. Puig, F. Sandiumenge, X. Obradors, J. Rabier, Microstructural influence on critical currents and irreversibility line in melt-textured $YBa_2Cu_3O_{7-x}$ reannealed at high oxygen pressure. *Phys. Rev. B* **65** (2002) 104526.

¹⁶ L. Mei, V.S. Boyko, S.-W. Chan, Twin engineering for high critical current densities in bulk $YBa_2Cu_3O_{7-x}$. *Physica C* **439** (2006) 78–84.

¹⁷ L. Mei, S.-W. Chan, Enthalpy and entropy of twin boundaries in superconducting $YBa_2Cu_3O_{7-x}$. *J. Appl. Phys.* **98** (2005) 033908.

¹⁸ A. Joulain, F. Sandiumenge, N. Vilalta, T. Prikhna, A.V. Vlasenko, J. Rabier, Dislocation configurations in twin free melt-textured $YBa_2Cu_3O_7$ processed at high pressure and high temperature. *Phil. Mag. Lett.* **8** (2005) 405–414.

¹⁹ V.S. Boyko, S.-W. Chan, Microstructure design by twinning in high-temperature superconductor $YBa_2Cu_3O_{7-\delta}$ for enhanced J_c at high magnetic fields. *Physica C* **466** (2007) 56–60.

²⁰ T.A. Prikhna, J. Rabier, A. Prault, X. Chaud, W. Gawalek, A.V. Vlasenko, J.-L. Soubeyroux, R. Tournier, F. Sandiumenge, Ya.M. Savchuk, V.E. Moshchil, P.A. Nagorny, N.V. Sergienko, V.S. Melnikov, S. Kracunovska, D. Litzkendorf, S.N. Dub, Structure and properties of melt-textured $YBa_2Cu_3O_{7-\delta}$, high pressure–high temperature treated and oxygenated under evaluated oxygen pressure. *Superconductor Sci. Technol.* **17** (2004) S515–S519.

²¹ T. Prikhna, X. Chaud, W. Gawalek, J. Rabier, Ya. Savchuk, A. Joulain, A. Vlasenko, V. Moshchil, N. Sergienko, S. Dub, V. Melnikov, D. Litzkendorf, T. Habisreuther, V. Sverdun, Oxygenation of the traditional and thin-walled MT-YBCO in flowing oxygen and under high evaluated oxygen pressure. *Physica C* **460–462** (2007) 392–394.

²² T.A. Prikhna, W. Gawalek, Ya.M. Savchuk, V.M. Tkach, N.I. Danilenko, M. Wendt, J. Dellith, H. Weber, M. Eisterer, V.E. Moshchil, N.V. Sergienko, A.V. Kozyrev, P.A. Nagorny, A.P. Shapovalov,

The working temperature of magnesium diboride can be chosen to be near that of liquid hydrogen or neon (20–30 K). It is easily produced and comparatively cheap, but prone to quenching during pulsed magnetization. This problem has to be solved in order not to restrict the material's widespread application. The working temperature of YBCO-based materials can be higher (e.g., around the temperature of liquid nitrogen, 77 K, or somewhat lower), but their production is much more expensive and complicated and the problems with a.c. losses and appropriate optimal twisting of coated conductor taps are not solved yet. A big risk of quenching and damaging powerful magnets exists for coated conductors as well.

Nowadays, investigations aimed at improving the characteristics of MgB₂-based materials and MT-YBCO look at the positive effect of oxygen in their structures on superconducting characteristics.^{28–32} Correlations between the character of the material inhomogeneities (which can be pinning centres) and the attained SC characteristics are considered in this paper.

2. Experimental

The preparation of MT-YBCO ceramics comprises two main stages: (1) formation (using an Sm123 seed crystal) of a pseudo-single domain YBa₂Cu₃O_{7- δ} ($\delta \approx 0.7$) block with finely dispersed inclusions of Y₂BaCuO₅ (Y211); (2) oxygenation of the YBa₂Cu₃O_{7- δ} matrix up to

-
- V.S. Melnikov, S.N. Dub, D. Litzkendorf, T. Habisreuther, Ch. Schmidt, A. Mamalis, V. Sokolovsky, V.B. Sverdun, F. Karau, A.V. Starostina, Higher borides and oxygen-enriched Mg–B–O inclusions as possible pinning centers in nanostructural magnesium diboride and the influence of additives on their formation. *Physica C* **470** (2010) 935–938.
- ²³ A.G. Mamalis, E. Hristoforou, I.D. Theodorakopoulos, T.A. Prikhna, Critical current density investigations of explosively compacted and extruded powder-in-tube MgB₂ superconductors. *Superconductor Sci. Technol.* **23** (2010) 095011.
- ²⁴ T.A. Prikhna, W. Gawalek, V.M. Tkach, N.I. Danilenko, Ya.M. Savchuk, S.N. Dub, V.E. Moshchil, A.V. Kozyrev, N.V. Sergienko, M. Wendt, V.S. Melnikov, J. Dellith, H. Weber, M. Eisterer, Ch. Schmidt, T. Habisreuther, D. Litzkendorf, J. Vajda, A.P. Shapovalov, V. Sokolovsky, P.A. Nagorny, V.B. Sverdun, J. Kosa, F. Karau, A.V. Starostina, Effect of higher borides and inhomogeneity of oxygen distribution on critical current density of undoped and doped magnesium diboride. *J. Phys.: Conf. Ser.* **234** (2010) 012031.
- ²⁵ T.A. Prikhna, W. Gawalek, Ya.M. Savchuk, N.V. Sergienko, V.E. Moshchil, V. Sokolovsky, J. Vajda, V.N. Tkach, F. Karau, H. Weber, M. Eisterer, A. Joulain, J. Rabier, X. Chaud, M. Wendt, J. Dellith, N.I. Danilenko, T. Habisreuther, S.N. Dub, V. Meerovich, D. Litzkendorf, P.A. Nagorny, L.K. Kovalev, Ch. Schmidt, V.S. Melnikov, A.P. Shapovalov, A.V. Kozyrev, V.B. Sverdun, J. Kosa, A.V. Vlasenko. Nanostructural superconducting materials for fault current limiters and cryogenic electrical machines. *Acta Phys. Polonica A* **117** (2010) 7–14.
- ²⁶ X. Chaud, J. Noudem, T. Prikhna, Y. Savchuk, E. Haanappel, P. Diko, C.P. Zhang, Flux mapping at 77 K and local measurement at lower temperature of thin-wall YBaCuO single-domain samples oxygenated under high pressure. *Physica C* **469** (2009) 1200–1206.
- ²⁷ T.A. Prikhna, M. Eisterer, M. Rindfleisch, A.V. Kozyrev, A.V. Shaternik, V.E. Shaternik, M. Tomsic, V.E. Moshchil, M.V. Karpets, V.B. Sverdun, S.S. Ponomaryov, V.V. Romaka, P.P. Seidel. MgB₂ wires and bulks with high superconductive performance. *IEEE Trans. Appl. Superconductivity* **29** (2019) 6200905.
- ²⁸ V. Solovyov, P. Farrell, Exfoliated YBCO filaments for second-generation superconducting cable. *Superconductor Sci. Technol.* **30** (2017) 014006.
- ²⁹ T.A. Prikhna, M. Eisterer, M. Rindfleisch, V.V. Romaka, M. Tomsic, V.E. Moshchil, M.V. Orlovsky, M.V. Karpets, V.B. Sverdun, S.S. Ponomaryov, A.V. Shaternik, A.V. Kozyrev, Correlations between superconducting characteristics and structure of MgB₂-Based materials, *ab-initio* modeling. *IEEE Trans. Appl. Superconductivity* **29** (2019) 2874415.
- ³⁰ T.A. Prikhna, M. Eisterer, A.V. Shaternik, V.E. Shaternik, P. Seidel, V. Sokolovsky, V.E. Moshchil,

$\delta \sim 0.1-0.0$, during which dislocations, stacking faults and twins (which, it is considered, can improve the SC properties, being pinning centres) and microcracks and macrocracks (harmful for SC current flow) can be formed. Three types of starting MT-YBCO have been used: Type 1 is a traditional bulk MT-YBCO produced from a mixture of commercial YBa₂Cu₃O_{7- δ} powder (Solvay) with Y₂O₃ and CeO₂ powders taken in the ratio of Y_{1.5}Ba₂Cu₃O_{7- δ} +1% CeO₂, the texturing process using seed crystals being carried out in the air.³³ Type 2 is thin-walled MT-YBCO with a set of parallel holes (Fig. 1a) (to reduce the depth of oxygen penetration during oxygenation), which has been obtained³⁴ from a mixture of 70 wt% of YBa₂Cu₃O_{7- δ} and 30 wt% of Y₂BaCuO₅, to which 0.15 wt% of PtO₂ has been added. The cooling of Type 2 MT-YBCO from 980 °C after formation of the Y123 took place in a low-oxygen atmosphere (below 0.5 kPa) with 0.1 MPa nitrogen in order to prevent cracking. The starting MT-YBCO samples of Types 1 and 2 had a tetragonal textured structure of the YBa₂Cu₃O_{7- δ} matrix with $\delta \approx 0.7$. Oxygenation was carried out under flowing oxygen at atmospheric pressure and under elevated oxygen pressure of up to 16 MPa. MT-YBCO after melt texturing was oxygenated at 440 °C in O₂ flow for 14 days and at 800 °C, 16 MPa O₂ for 3 days. The heating process in the case of oxygenation at 16 MPa was started in nitrogen at 0.1 MPa; it was gradually replaced by oxygen upon raising the temperature (to prevent oxygenation at low temperature and crack formation). After reaching the highest temperature the oxygen pressure was gradually increased up to 16 MPa.²¹ Type 3 MT-YBCO was obtained by high (mechanical quasihydrostatic) pressure–high temperature treatment^{20,35} of previously fully oxygenated (at 0.1 MPa flowing oxygen and 440 °C) MT-YBCO of Type 1. The high-pressure treatment was undertaken in contact with precompacted hexagonal ZrO₂ powder at 2 GPa, 800 °C for 0.5 h. Heating in contact with ZrO₂ at this pressure allows us to preserve oxygen content in the Y123 matrix.

Different forms of MgB₂-based materials were studied: thin films obtained by magnetron sputtering (a); bulk specimens synthesized from Mg:2B mixtures: at ambient pressure in Ar flow; (b) under high quasihydrostatic 2 GPa pressure (using amorphous boron without and with specially added carbon) (c); by spark plasma sintering under 50 MPa pressure (d); by hot

A.P. Shapovalov, V.V. Romaka, V.V. Kovylaev, S.S. Ponomaryov, Preparation and properties of MgB₂ thin films. *IEEE Trans. Appl. Superconductivity* **28** (2018) 7501507.

³¹ Y. Yang, M. Sumption, E.W. Collins, Influence of metal diboride and Dy₂O₃ additions on microstructure and properties of MgB₂ fabricated at high temperatures and under pressure. *Sci. Rep.* **6** (2016) 29306.

³² T. Prikhna, M. Eisterer, X. Chaud, H.W. Weber, T. Habisreuther, V. Moshchil, A. Kozyrev, A. Shapovalov, W. Gawalek, M. Wu, D. Litzkendorf, W. Goldacker, V. Sokolovsky, V. Shaternik, J. Rabier, A. Joulain, G. Grechnev, V. Boutko, A. Gusev, A. Shaternik, P. Barvitskiy, Pinning and trapped field in MgB₂ and MT-YBaCuO bulk superconductors manufactured under pressure. *J. Phys.: Conf. Ser.* **695** (2016) 012001.

³³ D. Litzkendorf, T. Habisreuther, J. Bierlich, O. Surzhenko, M. Zeisberger, S. Kracunovska, W. Gawalek, Increased efficiency of batch-processed melt-textured YBCO. *Superconductor Sci. Technol.* **18** (2005) S206.

³⁴ X. Chaud, D. Bourgault, D. Chateigner, P. Diko, L. Porcar, A. Villaume, A. Sulpice, R. Tournier, Fabrication and characterization of thin-wall YBCO single-domain samples. *Superconductor Sci. Technol.* **19** (2006) S590–S600.

³⁵ T.A. Prikhna, V.S. Melnikov, V.V. Kovylaev, V.V. Moshchil, Structural variations in high-temperature superconductive YBa₂Cu₃O_{7- δ} ceramic samples under high pressure–high temperature conditions. *J. Mater. Sci.* **30** (1995) 3662–3667.

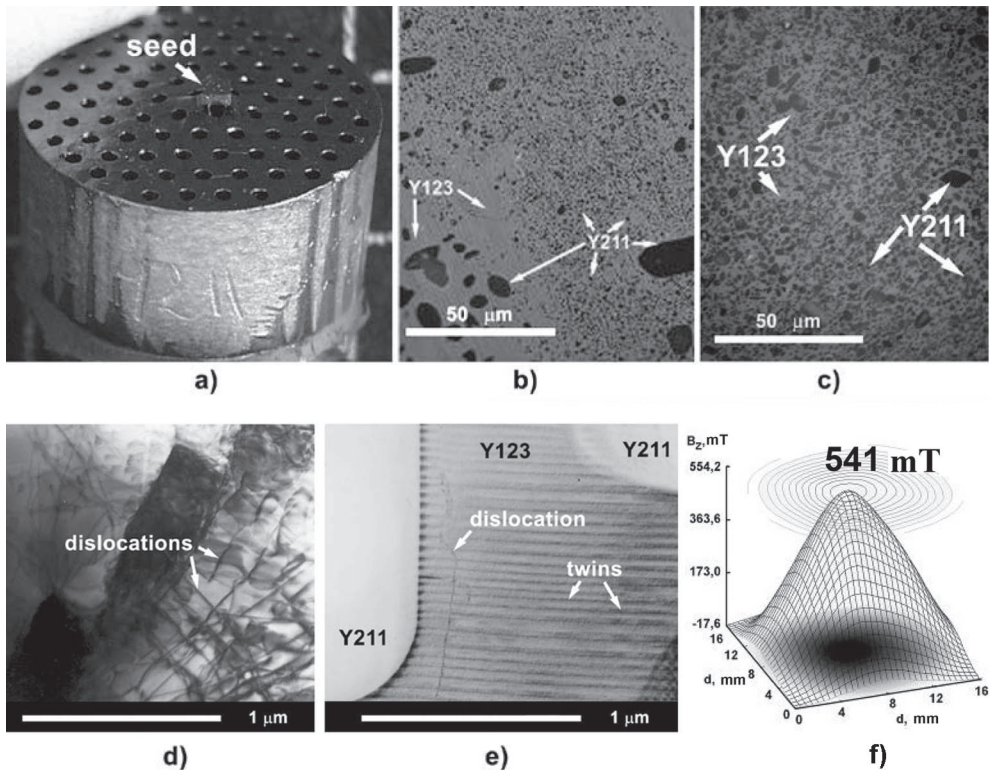


Figure 1. a) general view of thin-walled MT-YBCO of Type 2; b) and c) structure of MT-YBCO materials before oxygenation of Types 1 and 2, respectively, obtained via polarized light microscopy; d) dislocations in Type 3 detwinned MT-YBCO after high pressure treatment (image obtained by TEM); e) twins in Type 2 MT-YBCO in which dislocations were practically absent (image obtained by TEM); f) trapped magnetic fields (surface induction at 77 K after field cooling under 2 T) of thin-walled MT-YBCO of Type 2 oxygenated at 16 MPa (blocks 16 mm in diameter, 10 mm in height, with 0.8 mm holes).

pressing at 30 MPa (e); and wires prepared by HyperTech (by the authors of this paper) from Mg and B without and with C addition and without and with Dy₂O₃ additions (f).^{27,29,30}

Monofilamentary MgB₂ strands (wires) of round (0.83 mm in diameter) and quadratic (0.73 × 0.73 mm) cross-sections were sintered at 650 °C for 1 h. The strand architecture consists of a Monel outer sheath and a Nb barrier surrounding the powder mixture. The starting powders were undoped and C-doped boron from Specialty Materials Inc. (SMI). The boron powders from SMI were mostly amorphous with a particle size of 10–100 nm. The C-doped powders contained 2 mol% C. The round wire with the addition of 4 wt% of Dy₂O₃ nanopowders to the Mg:2B mixture was prepared using C-doped boron.

The MgB₂ bulk samples were prepared in MgB₂ stoichiometry without and with carbon addition. The high pressure (2 GPa)–high temperature (600–1050 °C) synthesis of bulk MgB₂ was carried out in contact with precompacted hexagonal boron nitride powder in a recessed-anvil high-pressure apparatus.³⁵ They were prepared by spark plasma sintering as well: under 50 MPa pressure, at 600 °C for 0.3 h and at 1050 °C for 0.5 h from a mixture of Mg and B

powders with MgB₂ stoichiometry. Thin films of MgB₂ (about 140±10 nm thick) were deposited on 8×8×0.2 mm sapphire substrates with (001) orientation. The deposition was made by magnetron sputtering in an Ar atmosphere at a pressure of about 1 Pa using a MgB₂ hot-pressed target. *In situ* annealing of the deposited films was carried out subsequently.³⁰

Structure was examined using polarized optical microscopy and a TEM (200 kV) as well as X-ray diffraction (with Rietveld refinement) and SEM with microprobe X-ray and Auger (JAMP[®]9500F) options.

The critical current densities (j_c) of bulk and films were obtained from magnetization measurements in an Oxford Instruments 3001 vibrating sample magnetometer (VSM) using the Bean model. The critical current density of wires was defined by the commonly used electric field criterion, $E_c = 1 \mu\text{V cm}^{-1}$, when the electric field during ramping the current (and the current density J) exceeds this value, i.e. $J_c = J(E_c)$. The constant offset voltage caused by induction was subtracted before data processing.

For investigation of the oxygenation process of MT-YBCO after texturing (before oxygenation), small rectangular bars with dimensions of about 2×2×5–7 mm were cut from the MT-YBCO blocks (Types 1 and 2) oriented such that the longer sides of the bars were parallel to the c -axis of the Y123 matrix and perpendicular to its ab -planes. It was possible because the position and orientation of the seed crystal used for the manufacture of the melt-textured quasi-single domain block was known. Small samples (rectangular bars) of Types 1 and 2 and melt-textured large blocks were simultaneously oxygenated under the same conditions. The number of cracks was calculated for the entire small samples using polarizing microscopy. Linear densities of cracks were calculated using dozens of separate images collected together, which revealed the numbers of cracks on the entire surfaces of the rectangular bars. After polishing, macrocracks became visible and after etching by acid the microcracks became visible as well. Cracks are usually parallel to the ab -planes because they appear during oxygenation due to the decreasing c -parameter. The density of twins was estimated by polarized light microscopy and TEM. The trapped fields were studied by scanning with a Hall probe surfaces of the big whole blocks oxygenated together with small rectangular bars after their field cooling. Hardness was measured with a Matsuzawa MXT-70 microhardness tester for H_V (using a Vickers indenter). Fracture toughness was estimated from the length of the radial cracks emanating from the corners of an indentation.

3. Results and discussion

3.1 MT-YBCO

Analysing the data given in Table 1 one can see that the density of twins correlates with distance between Y211 inclusions (Fig. 1, b & c) and critical current densities. TEM showed that shorter distances between Y211 grains resulted in a higher density of twins.³² According to X-ray structural analysis, the YBa₂Cu₃O_{7- δ} matrices of all the materials investigated in this paper were fully oxygenated with $7-\delta \approx 6.9-7.0$. Despite the density of dislocations (Fig. 1d)—after high pressure–high temperature treatment it was increased by about 4 orders of magnitude, reaching 10^{12} cm^{-2} —and the many stacking faults present, the parallel detwinning leads to low critical currents (Table 1). Thus, MT-YBCO material with a high concentration of dislocations in the

YBa₂Cu₃O₇ phase but with very low twin density manifests a critical current density essentially lower than that without dislocations and stacking faults, but with a high concentration of twins (Fig. 1e). The more homogeneously distributed Y211 grains in Y123 matrices with short distances between them in Type 2 MT-YBCO lead to a higher twin density after oxygenation at high pressure (16 MPa), which allowed us to obtain an extremely high irreversibility field of 9.7 T at 77 K in the *ab*-plane ($H||c$). The oxygenation at elevated isostatic pressure and temperature higher than 750 °C leads not only to high twin density in the Y123 structure but practically to the absence of dislocation and stacking faults in it (Fig. 1e).

Table 1. Characteristics of MT-YBaCuO of Types 1–3 oxygenated under different conditions (in all the cases the YBa₂Cu₃O_{7- δ} matrices were fully oxygenated ($7-\delta \approx 7$)).

Type 1		Type 2		Type 3
0.1 MPa, 440 °C	16 MPa, 800 °C	0.1 MPa, 440 °C	16 MPa, 800 °C	0.1 MPa, 440 °C and 2 GPa, 800 °C
Density of microcracks/mm ⁻¹				
890	200	1500	270	-
Density of twins/ μm^{-1}				
0.5–15	7–20	12–16	20–35	0–1
Density of macrocracks/mm ⁻¹				
1.5	0.4	1.3	absent	-
Critical current density at 0 T field/kA cm ⁻²				
$H c$				
58.0	83.0	60.0	81.0	9.2
$H ab$				
16.5	30.0	17.5	34.0	4.2
Irreversibility field/T ($H c$)				
6.3	5.8	8.7	9.7	5.7
Vickers microhardness (H_v)/GPa, estimated at $P=4.9$ N				
on <i>ab</i>				
4.3±1.1	6.3±0.5	6.8±0.9	7.3±0.2	-
$\perp ab$				
6.6±0.5	7.5±0.6	7.6±0.1	7.6±0.3	-
Fracture toughness (K_{Ic})/MPa m ^{0.5} , estimated at $P=4.9$ N				
on <i>ab</i>				
0.7±0.2	3.31±1.05	1.9±1.4	4.37±0.77	-
$\perp ab$				
-	1.95	1.73±0.13	2.8±0.24	-

The high pressure (16 MPa)–high temperature (800 °C) oxygenation allowed the number of microcracks to be decreased and practically excludes macrocracks parallel to the *ab*-plane, which in turn leads to an increase of critical current density in the *c*-direction and to a reduction of critical current density anisotropy. The observed increase of the Vickers hardness for the *ab*-plane can be connected with twin density increase and with reduction of the number of microcracks, which are usually parallel to the *ab*-planes (Table 1). The observed increase of the fracture toughness may have a similar explanation. The formation of twins is connected with the transformation of tetragonal YBa₂Cu₃O_{7- δ} into orthorhombic structures and thus with

increasing oxygen concentration in the basal planes from 6.3 to 7 atoms per unit cell (during which the c -parameter diminishes). Elevated pressure (10–16 MPa) is necessary to keep oxygen in the Y123 structure at high temperature (800 °C). Since the diffusion rate increases at high temperature and the oscillations of atoms around their positions in the crystal lattice increase, oxygen under enhanced pressure can enter the $YBa_2Cu_3O_{7-\delta}$ tetragonal structure with lower resistance. This can explain the diminution of cracking during oxygenation at high temperature and isostatic elevated oxygen pressure.

The trapped field of the thin-walled MT-YBCO sample estimated using the block 16 mm in diameter and 10 mm in height with 0.8 mm diameter holes is shown in Fig. 1f. The maximal trapped field value of 0.54 T was observed after short-time oxygenation at 800 °C at 16 MPa oxygen pressure.

3.2 MgB_2 -based materials

Despite magnesium diboride being nominally an oxygen-free compound it is practically impossible to synthesize or sinter materials based on it without oxygen impurities, because of the high affinity of Mg for oxygen. Recently we have shown that superconducting matrices of bulk magnesium diboride with AlB_2 structures contain some oxygen in their unit cells ($MgB_{1.68-1.8}O_{0.32-0.2}$).²⁹ This was shown experimentally by X-ray and Auger studies and supported by *ab initio* simulation. Materials with such matrices demonstrated extremely high superconductivity.^{27,29}

The typical microstructures of MgB_2 -based bulk material, thin films and wires that demonstrated good SC characteristics are shown in Fig. 2. The dependences of critical current densities v . magnetic fields are presented in Figs 3 and 4. The structures of all the investigated materials were not homogeneous; periodically repeated nano- or micro-sized zones of different compositions can be the reason for strong pinning³⁶ and high critical currents. Admixed oxygen seems to play an important role in attaining strong pinning because it preferentially segregates, forming separate Mg–B–O oxygen-enriched inclusions (in Fig. 2f, Mg-B-O inclusions appear white or bright) or nanolayers (Fig. 2e, marked by “A”, and appear the brightest). MgB_2 -based bulk materials obtained at lower temperatures (600–800 °C) usually yield less segregated admixed oxygen (it forms Mg-B-O nanolayers), while materials prepared at higher temperatures contain separate Mg-B-O inclusions.²⁹ Some additives (Ti, Ta, Zr, SiC) also promote an increase of admixed oxygen aggregation and lead to the formation of separate inclusions even at comparatively low synthesis temperatures (800 °C).³⁷ The results of *ab initio* calculations of the electronic structure and stability of magnesium diboride compounds with partial oxygen or carbon substitution for boron show that it is energetically favourable in the MgB_2 structure for oxygen to replace boron pairwise in neighbouring positions or to form zigzag chains, and for carbon atoms to be distributed homogeneously³⁸ (i.e., it is favourable for

³⁶ M. Eisterer, Calculation of the volume pinning force in MgB_2 superconductors. *Phys. Rev. B.* **77** (2008) 144524.

³⁷ T. Prikhna, Structure and properties of bulk MgB_2 . In: *MgB₂ Superconducting Wires* (ed. R. Flükiger) (World Scientific Series in Applications of Superconductivity and Related Phenomena Vol. 2), ch. 3a (pp. 131–157). Singapore: World Scientific (2016).

³⁸ T.A. Prikhna, A.P. Shapovalov, G.E. Grechnev, V.G. Boutko, A.A. Gusev, A.V. Kozyrev, M.A. Belogolovskiy, V.E. Moshchil, V.B. Sverdun, Formation of nanostructure in magnesium diboride-based materials with high superconducting characteristics. *Low Temperature Phys.* **42** (2016) 380–394.

oxygen atoms to aggregate). It is considered that the boundaries between areas with any deviation in concentration or such zones (inclusions) themselves are potentially places for pinning Abrikosov vortices. Zones with essentially a higher concentration of boron than in MgB₂ (so-called higher magnesium borides, MgB_y, $y > 6$) appeared the blackest (see, e.g., Fig. 2f), can also affect pinning and their augmented presence in the structure usually leads to an increase of critical current density in high magnetic fields.

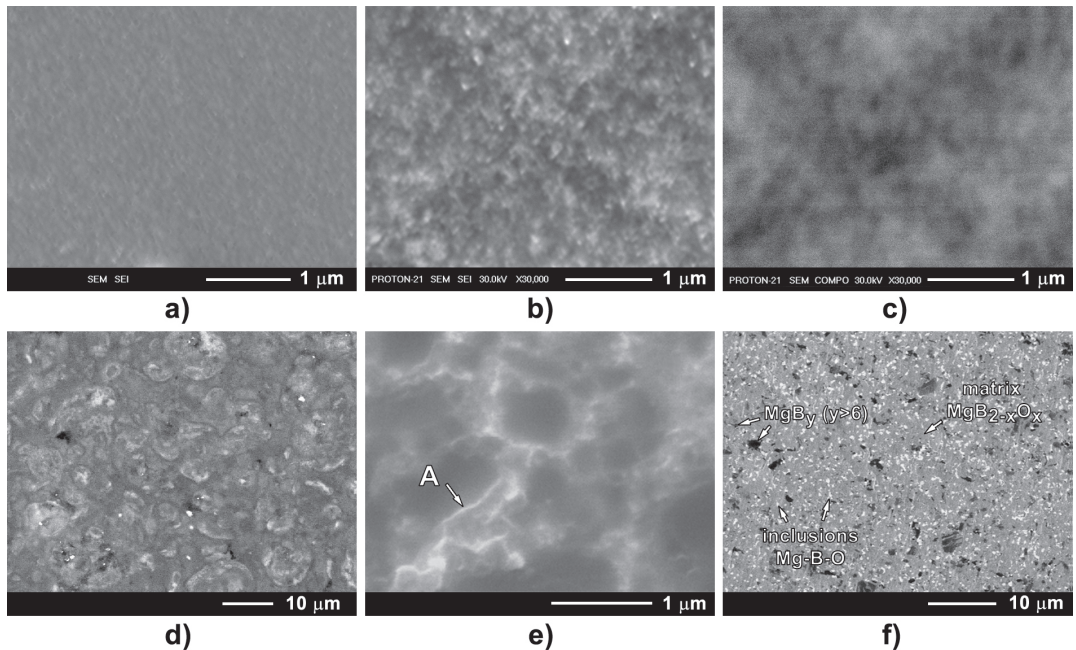


Figure 2. Microstructures of MgB₂-based materials, obtained by SEM, of: a) thin film secondary electron image (SEI), its j_c dependences are shown in Fig. 4, curves 5 and 6; b) and c) wire (same place under the same magnification in SEI and BEI, respectively), its j_c at 4.2 and 20 K are shown in Fig. 5, curve 4); d), e) and f) bulk materials backscattered electron image (BEI), synthesized, respectively, from: Mg:2B using C-doped amorphous B at 600 °C, 2 GPa, 1 h, its j_c shown in Fig. 4, curve 2; Mg:2B using boron without carbon at 800 °C, 2 GPa, 1 h; and Mg:2B using B without carbon at 1050 °C, 2 GPa, 1 h.

Fig. 3 demonstrates the critical current density dependences $v.$ applied magnetic fields at 20 K estimated magnetically (using a vibrating sample magnetometer and the Bean model) for bulk MgB₂-based materials prepared under different pressures (created using different methods of synthesis, curves 1–4) and in two directions (parallel and perpendicular to the film surface, curves 6 and 5) for thin films obtained by magnetron sputtering. The finer nanostructural inhomogeneities in the thin film (Fig. 2a) lead to higher critical currents (Fig. 3, curve 6) in comparison with wires (Fig. 4) and bulk samples (Figs 2b–f; Fig. 3, curves 1–4).

The data represented by curves 1, 3 and 4 in Fig. 3 evidence the positive effect of pressure applied during synthesis. This is not only due to the possibility to attain a denser structure but also because of suppression of Mg's volatility. The combination of high pressure and addition of carbon to boron allowed us to essentially increase the critical current density in high magnetic fields, while due to a decrease of the superconducting transition temperature (from

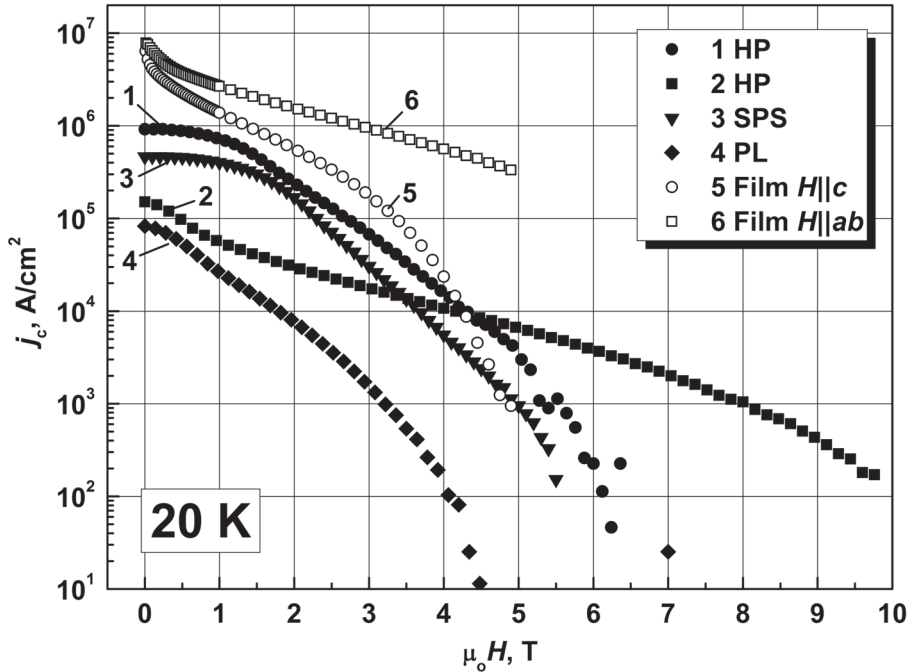


Figure 3. Dependences of critical current density, j_c , v. magnetic field, $\mu_0 H$, estimated at 20 K for MgB_2 -based materials. Key: 1 HP high-pressure, synthesized at 2 GPa, 1050 °C, 1 h from Mg and B with MgB_2 stoichiometry; 2 HP high-pressure, synthesized at 2 GPa, 600 °C, 1 h from Mg and B (with C addition) with MgB_2 stoichiometry; 3 SPS spark-plasma synthesized at 50 MPa, 600 °C for 0.3 h and at 1050 °C for 0.5 h from Mg and B with MgB_2 stoichiometry; 4 PL pressureless sintering at 0.1 MPa (1 atm in flowing Ar), 800 °C, 2 h from a precompact mixture of Mg and B with MgB_2 stoichiometry; 5 Film $H||c$ and 6 Film $H||ab$ are thin films deposited by magnetron sputtering, with the magnetic field parallel and perpendicular to the film surface, respectively.

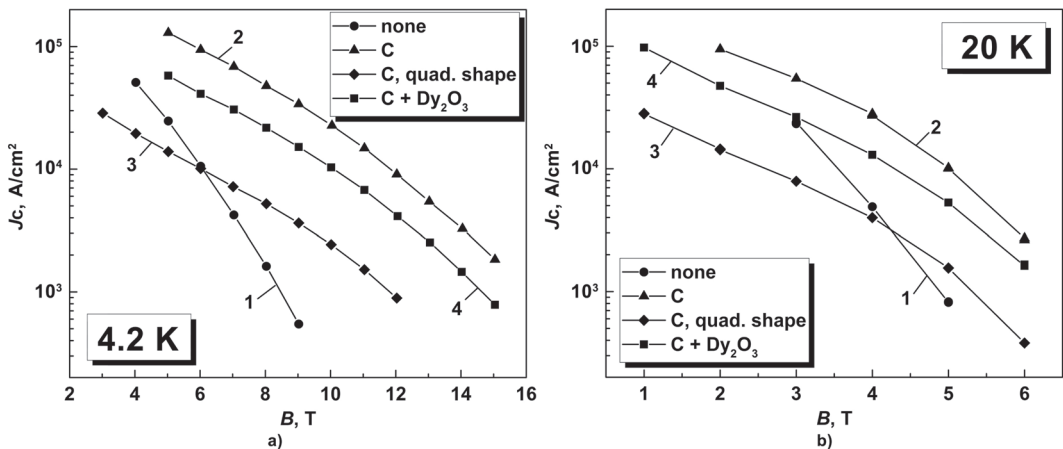


Figure 4. Critical current densities of wires at a) 4.2 K and b) 20 K. The solid lines are merely a visual guide.

38.2 down to 35 K because of carbon incorporation into the MgB₂ lattice) the critical current decreased in low magnetic fields (Fig. 3, curve 2).

Figs 5 and 6 present the results of the structural study by SEM and EDX of single filamentary strands or wires manufactured from Mg and B without additions (Fig. 5) and with the addition of 2 mol% of C (Fig. 6). Figure 6c shows the structure of a wire prepared from a mixture of Mg and B with 2 mol% of C taken in Mg:2B's stoichiometry, to which 4 wt% of Dy₂O₃ nanopowder was added as well. The results of critical current density estimation v. magnetic field at 4.2 and 20 K of wires prepared from boron with carbon addition are presented in Fig. 4. The highest critical current flowed in round wire prepared using boron with carbon addition (curves 2, Figs 4a and b); wire with added Dy₂O₃ nanopowder (curves 4, Figs 4a and b) were somewhat lower. The lowest critical currents were in wire of square cross-section prepared from boron with carbon addition (curves 3, Figs 4a and b), while all technological aspects except shaping were absolutely the same as in the case of the round wire (curves 2).

The structural study (Figs 5 and 6) after deep Ar ion etching of the surfaces of the wire (to remove the surface oxidized layer) in the chamber of a microscope allowed us to conclude that all wires contained a rather high amount of oxygen. Hence, admixed or specially added (in the case of Dy₂O₃) oxygen is not the obstacle for attaining high critical currents in MgB₂ wires. Table 2 summarizes the results of the SEM EDX study of deviation from stoichiometry and presents average compositions of the main matrix phases of wires. In the wire with added Dy₂O₃, dysprosium or a dysprosium-containing phase was only found in several localized spots (see, e.g., Fig. 6c, point S4), hence distributed quite inhomogeneously, enacting pinning in the MgB₂-based wire. The average amount of oxygen and the carbon concentration were practically the same in the matrices of square-shaped wire without (№ 3) and round-shaped wire with (№ 4) additions of Dy₂O₃, while the amount of boron in the last wire was essentially higher than needed according to the MgB₂ stoichiometry (Table 2). The microstructure of the square-shaped wire (Fig. 6b and № 4 in Table 2) was very inhomogeneous, while the microstructure of round wire prepared from the same initial powdered mixture turned out to be very homogeneous (Fig. 6a and № 2 in Table 2) and contained the lowest amount of admixed oxygen than all the other wires examined. The average Mg:B ratio of the round wire (№ 2) was close to that of MgB₂ stoichiometry (MgB_{2,1}) and, in contrast to the square-shaped wire (№ 3), deviated from point to point in a very narrow range. Thus, the most reasonable explanation why their dependencies of critical current densities are so different (Fig. 5) can be the fact that the different styles of their drawing led to the difference in the homogeneity of their structures after sintering, especially, to the deviation of the Mg:B ratio. In the wire with Dy₂O₃ addition it was essentially shifted towards higher concentrations of boron (MgB_{3,6-5,2}) and the Dy-contained phase was not homogeneously distributed in the wire matrix (Table 2, № 4, Fig. 6c). It is well known from our previous studies of bulk magnesium diboride-based materials that even if the ratio between magnesium and boron in their matrices differs to high extent from MgB₂ stoichiometry (for example, if the material mainly contains MgB_y (12 > y > 6) phases), the absolute level of critical current density (estimated magnetically) can be comparatively high,²⁵ but still essentially lower than that of the material with near-MgB₂ stoichiometry of the matrix phase. Possibly, higher boron concentration (wire № 4) leads to some decrease in critical current density in comparison with the wire to which just carbon was specially added (wire № 2).

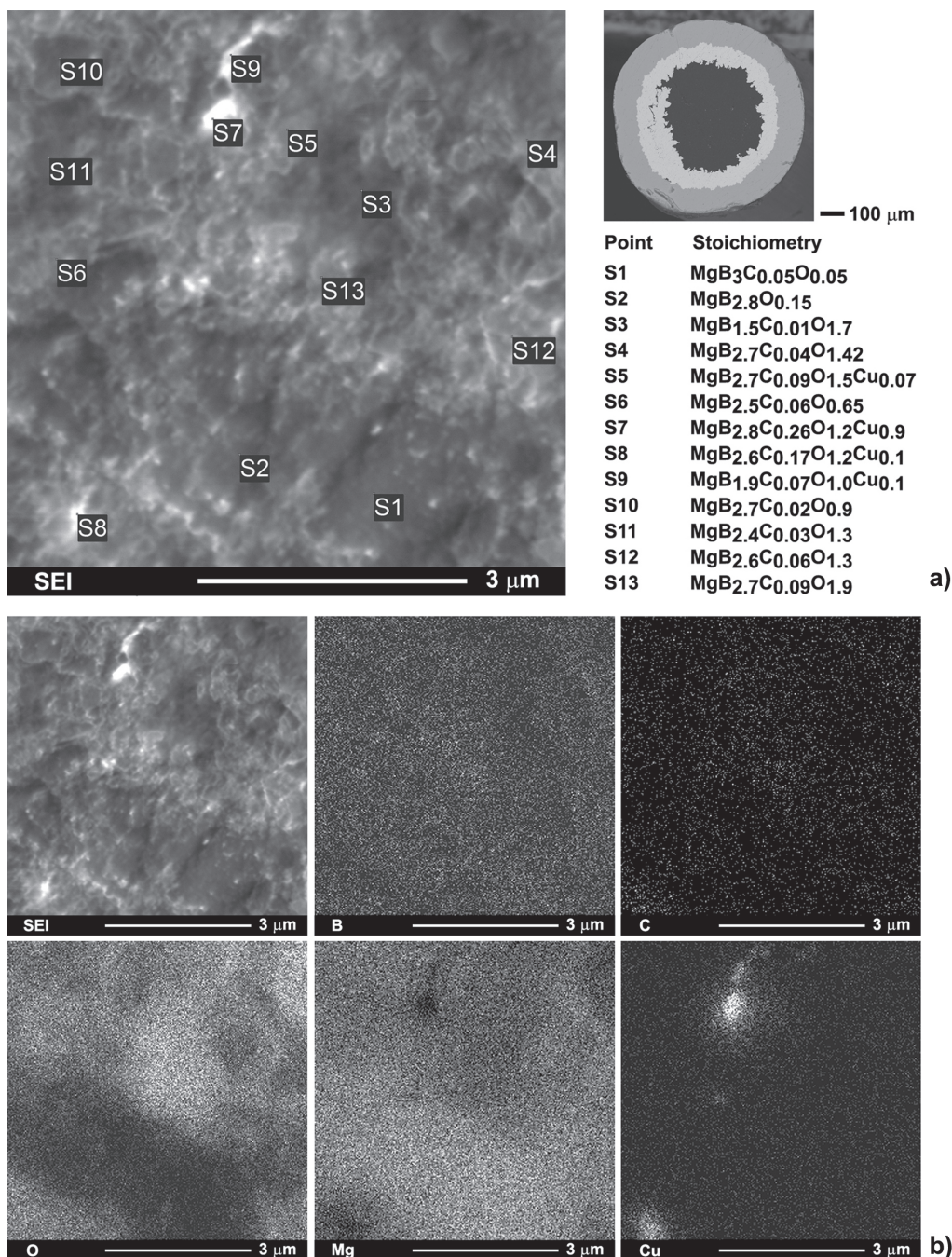


Figure 5. Microstructure of wire (strand) prepared from magnesium and boron without carbon addition (curves 1 in Fig. 4): (a) image of microstructure with points of analysis (SEI) and approximate stoichiometry in these points estimated using EDX analysis and image of cross-section of wire (BEI); (b) image of microstructure (SEI) and maps of B, C, O, Mg and Cu distributions on the area of image (obtained by SEM).

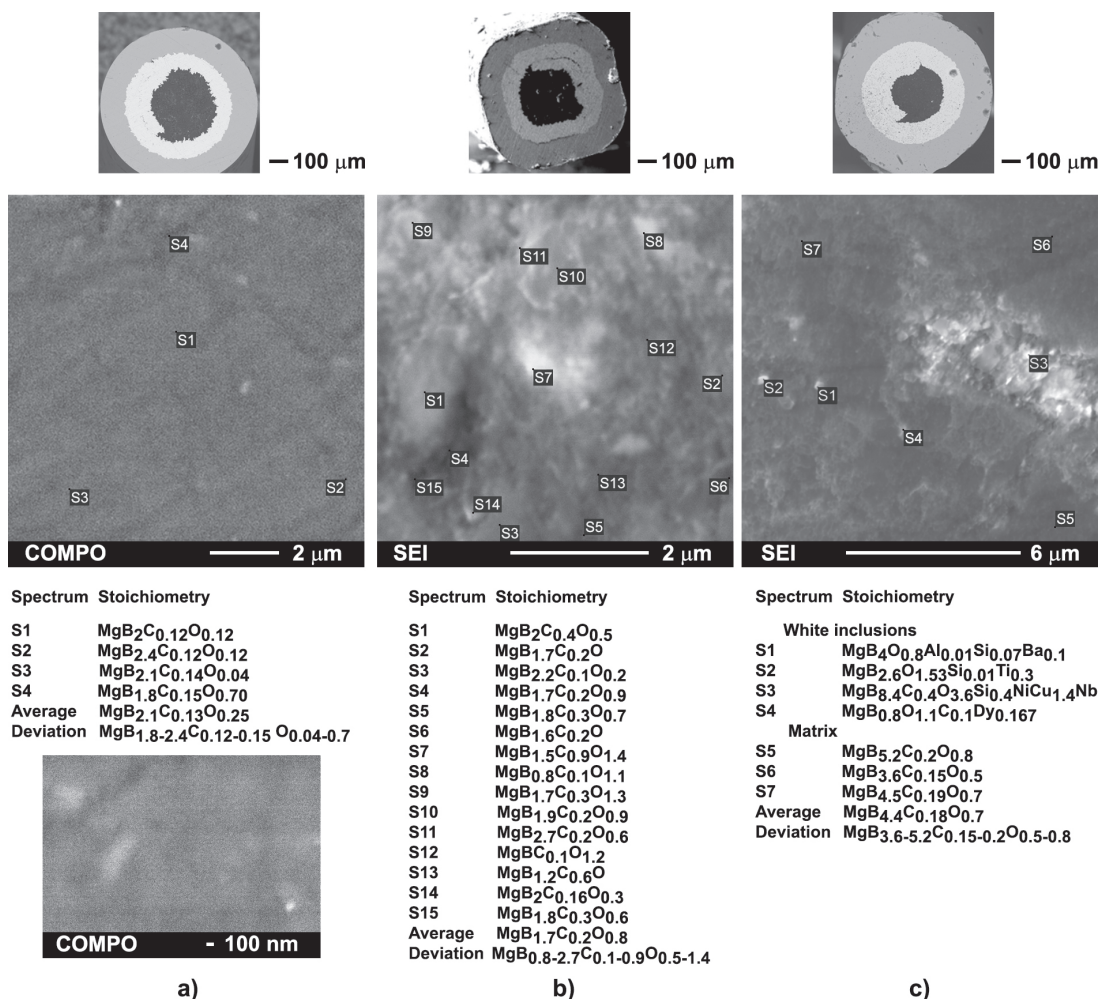


Figure 6. Images of cross-sections of wires (BEI) and microstructures (SEI and BEI) with points of analysis and approximate stoichiometry in these points estimated using EDX analysis: (a) round-shaped wire prepared using Mg and B (with 2 mol% C) and EDX results in points, after EDX results the wire microstructure (BEI) is given at higher magnification; (b) square-shaped wire prepared using Mg and B (with 2 mol% C); (c) round-shaped wire prepared using Mg and B (with 2 mol% C) and 4 wt% Dy₂O₃ additions to Mg:2B mixture.

Table 2. Deviation in stoichiometry and average composition of the main phase of different types of MgB₂-based wires.

Type of wire	Range of composition	Average composition
1. Mg:2B(without C), round shape	MgB _{1.5-2.7} C _{0.01-0.09} O _{0.65-1.9}	MgB _{2.3} C _{0.08} O _{1.3}
2. Mg:2B(with 2mol% C), round shape	MgB _{1.8-2.4} C _{0.12-0.15} O _{0.04-0.7}	MgB _{2.1} C _{0.13} O _{0.25}
3. Mg:2B(with 2mol% C), square shape	MgB _{0.8-2.7} C _{0.1-0.9} O _{0.5-1.4}	MgB _{1.7} C _{0.2} O _{0.8}
4. Mg:2B(with 2mol% C) + 4wt% Dy ₂ O ₃ , round shape	MgB _{3.6-5.2} C _{0.15-0.2} O _{0.5-0.8}	MgB _{4.4} C _{0.18} O _{0.7}

The wire prepared from boron without expressly added carbon (Fig. 6 and № 1 in Table 2) contained a small amount of admixed carbon after synthesis, which can originate from the initial amorphous boron (in which some impurity carbon can be present). Its microstructure was less homogeneous (Fig. 6) than that of wire prepared using boron with expressly added carbon (Fig. 6a) and contained a higher amount of admixed oxygen (compare nos 1 and 2 in Table 2). The lower concentration of carbon can be the reason of comparatively low critical current densities in high magnetic fields. The effect is well known and widely discussed in the literature.

Comparing structures and characteristics of different wires it is possible to conclude that for attaining high superconducting performance in high magnetic fields it is rather important to create a homogeneous structure with composition of the matrix near to MgB₂. The presence of oxygen is not an obstacle to attaining high SC characteristics. The distribution of oxygen may affect the critical current density. A more homogeneous structure is preferable. The Dy₂O₃ nanopowder was not homogeneously distributed in the round wire, so it is not easy to establish the reason for its somewhat lower SC characteristics than that of round wire prepared using the same carbon-doped boron but without the addition of Dy₂O₃. The comparison of SC characteristics of round wire with Dy₂O₃ addition (№ 4) and square wire (№ 3), which contained practically the same amounts of carbon and oxygen, evinced that for higher critical currents the somewhat higher (cf. MgB₂ stoichiometry) concentration of boron (MgB_{4.4}) in the matrix is less deleterious than somewhat lower (MgB_{1.7}).

4. Conclusions

The observed correlations between structures and SC characteristics of YBa₂Cu₃O_{7-δ} (MT-YBCO)- and MgB₂-based materials (wires, bulk material and thin films) promising for practical applications brought us to the conclusion that the amount and distribution of oxygen in their structures play an important role for pinning and superconducting properties. During oxygenation of the YBa₂Cu₃O_{7-δ} phase of MT-YBCO twins are forming due to variation of YBa₂Cu₃O_{7-δ} lattice parameters. The high density of twins together with a high density of fine Y₂BaCuO₅ inclusions and their homogeneous distribution in YBa₂Cu₃O_{7-δ} is extremely important for attaining high critical currents, because the places of twin intersection and places where twins intersect with Y₂BaCuO₅ inclusions can be pinning centres for superconducting vortices. The energetic advantages of oxygen aggregation in the MgB₂ structure lead to the formation of periodically repeated nanoscale areas with different oxygen concentrations, which can positively influence pinning. Besides, the boundaries between oxygen-enriched micro-sized areas can be responsible for the pinning increase as well. The MgB₂-based wires contain impurity oxygen and the homogeneity of their structures is of great importance for attaining high critical currents. Having the Mg:B ratio close to MgB₂ allows obtaining the highest critical currents; deviation towards higher boron concentrations seems less deleterious for superconducting performance than towards lower concentrations.

Acknowledgments

These investigations were carried out within the framework of project III-3-18 (0776) and contract ISM-29/20, supported by the National Academy of Sciences of Ukraine.